

DPF2015-22
May 8, 2022

Test of Lorentz Invariance from Compton Scattering

PRAJWAL MOHANMURTHY ¹

*Laboratory for Nuclear Science
Massachusetts Institute of Technology
77 Massachusetts Avenue, Bldg 26-568, MA 02139, U.S.A*

DIPANGKAR DUTTA, AMRENDRA NARAYAN ²

*Department of Physics and Astronomy
Mississippi State University
P. O. Box 5167, Mississippi State, MS 39762, U.S.A*

In the recent times, test of Lorentz Invariance has been used as a means to probe theories of physics beyond the standard model, especially those such as extensions to String Theory and Quantum Gravity. Tests of Lorentz invariance could go a long way in setting the stage for possible quantum gravity theories which are beyond the standard model. We describe a simple way of utilizing the polarimeters, which are a critical beam instrument at precision and intensity frontier nuclear physics labs such as Stanford Linear Accelerator Center (SLAC) and Jefferson Lab (JLab), to limit the dependence of speed of light with the energy of the photons. Furthermore, we also describe a way of limiting directional dependence of speed of light at previously unprecedented levels of precision by studying the sidereal variations. We obtain a limit of MSME parameters: $\sqrt{\kappa_X^2 + \kappa_Y^2} < 2.4 \times 10^{-17}$ and $\sqrt{(2c_{TX} - (\tilde{\kappa}_{0+}^{YZ})^2 + (2c_{TY} - (\tilde{\kappa}_{0+}^{ZX})^2} < 2.4 \times 10^{-17}$. We also obtain a leading value for the refractive index of free space $n = 1 + (0.18 \times 10^{-9} \pm 0.02 \times 10^{-9})$.

PRESENTED AT

DPF 2015

The Meeting of the American Physical Society
Division of Particles and Fields
Ann Arbor, Michigan, August 4–8, 2015

¹jprajwal@mohanmurthy.com; Now at ETH Zurich & Paul Scherrer Institute.

²Now at Indian Institute of Technology, Bombay.

1 Introduction

Lorentz invariance was first introduced in Special Relativity and then generalized in General Relativity to prevent infinities in self energies of Maxwellian Electro-Magnetic systems, but has formed the corner stone of modern standard model. Testing the Lorentz symmetry rigorously is thus a very interesting research activity. There are direct tests of Lorentz invariance mostly involving studying the dependence of speed of light on a number of other physical properties such as its energy, over distance of propagation and direction of propagation, to name a few. According to the CPT theorem, the joint Charge-Parity-Time symmetry has to hold for all processes governed by a Lorentz invariant theory and vice-versa [3]. Therefore, in particle and nuclear physics probing violations of CPT symmetry has been a means to test Lorentz invariance. Nuclear and particle physics methods often involve indirect tests of Lorentz invariance by measuring violations of CPT symmetry either by studying the joint CPT symmetry or by studying a subset of the CPT symmetry, such as CP symmetry violation or T symmetry violation independently.

Previous to the discovery of weak sector parity violation in beta decay experiment at NIST [1], it was assumed that parity was a conserved quantity. It was then assumed that CP was a conserved quantity until neutral kaon decay experiment proved otherwise [2]. Since then, CPT symmetry and Lorentz symmetry by extension, is shown to hold good in modern standard model. Certain beyond the standard model (BSM) theories have however been known to break CPT symmetry and Lorentz symmetry by extension. Ref. [4] lists all known BSM theories that break CPT and Lorentz symmetry as of publication date, while Ref. [5] lists all the experimentally measured parameters limiting the violation of CPT and Lorentz symmetry as of publication date.

Compton scattering, which is currently the only way of continuously monitoring electron beam polarization precisely has spawned Compton polarimeters at each of the labs using polarized electron beam to probe nuclear matter such as SLAC and JLab. These Compton polarimeters have recently been demonstrated to achieve precision as low as 1% [6]. The high degree of precision of Compton polarimeters allows precise measurement of speed of light competent with the current leading limits. Using a competent value of the speed of light so obtained, limits on SME parameters could be established.

2 Compton Polarimeter

At JLab, the electron beam helicity (\pm) is switched at the rate of 960Hz and the photon beam used for Compton scattering can be switched on or off (on/off). A term, scattering asymmetry (A_{exp}) can then be defined by measuring the cross section of

scattered electrons from Compton scattering.

$$A_{exp} = \frac{Y^+ - Y^-}{Y^+ + Y^-}$$

$$A_{exp} = P_\gamma P_e A_{phy} \quad (1)$$

where $Y^\pm = N_{on}^\pm/Q_{on}^\pm - N_{off}^\pm/Q_{off}^\pm$ so that backgrounds are subtracted when photon beam is turned off, $N_{on/off}^\pm$ is the cumulative number of scattered electrons detected at a strip and $Q_{on/off}^\pm$ is the cumulative main electron beam charge. P_γ is the polarization of the photons beam used and P_e is the polarization of the electron beam used. A_{phy} is the physics asymmetry which can be calculated as a function of a dimensionless variable, ρ [28].

$$\rho = \frac{\omega'}{\omega_{max}} \approx \frac{\epsilon_0 - \epsilon'}{\epsilon_0 + \epsilon'_{min}} \quad (2)$$

where ω' is the energy of the Compton scattered photon, ω_{max} is the maximum scattered photon energy, ϵ' , ϵ'_{min} and ϵ_0 are scattered electron energy, minimum scattered electron energy and main electron beam energy.

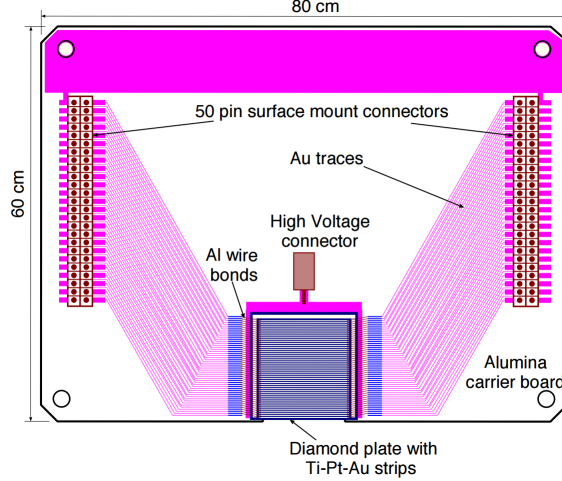


Figure 1: Picture of the multi-strip electron detector which is made of vapor deposited diamond.

Parity violating electron scattering experiments such as the QWeak experiment at JLab, which measured the weak mixing angle away from the Z^0 pole, rely heavily on the knowledge of electron beam polarization. The QWeak experiment at JLab demanded a polarimeter which could measure the average electron polarization to 1%

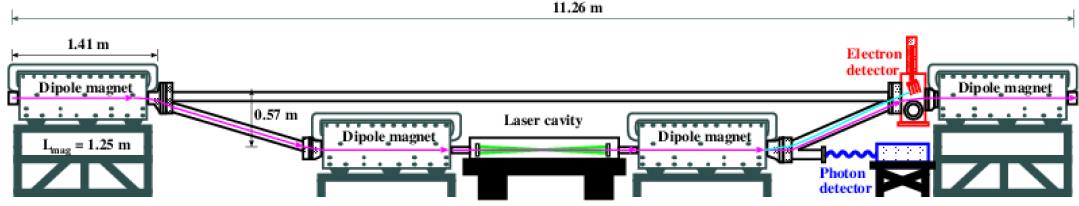


Figure 2: Sketch illustrating the 4-dipole (grey boxes) chicane used in Jlab Compton Polarimeter along with the photon and electron detectors. The blue line represents the electron beam while the yellow line represents the photon beam.

precision within an hour [15, 16]. Since Compton scattering is electron-polarization sensitive, it is a good means of measuring electron polarization. The new Hall-C Compton polarimeter achieves 1% precision in measured value of electron polarization in under an hour [6]. The JLab Hall-C polarimeter was installed on the beam line prior to the liquid hydrogen (QWeak) target and consists of 4 - dipole chicane where a photon beam interacts with the electron beam in a Fabry-Pérot cavity as illustrated in FIG. 2 [16]. Unlike the Möller polarimeter, the Compton polarimeter is non-invasive and continuous since it can be operated simultaneously with a scattering experiment.

Compton polarimeters use a well known technique of measuring electron beam polarization using Compton scattering with known photon polarization [17, 18, 19, 20, 21, 22, 23, 24]. The Compton scattered electrons and photons can be independently analyzed to obtain the electron beam polarization. Usually the photons have been analyzed to obtain electron beam polarization [17, 18, 19, 20, 21, 22, 23], but in recent times many experiments use analysis of scattered electrons to measure the electron beam polarization [25]. The scattered asymmetry increases with the electron beam energy. The QWeak experiment at JLab Hall-C only used 1 GeV electron beam and therefore it was much more challenging to obtain high degree of precision in electron polarimetry given the scattering asymmetry was just about 0.04. The small asymmetry means that a very high luminosity is required at the Compton scattering point. The high luminosity was obtained by locking and storing a 10W, 532nm laser in a Fabry Pérot cavity. This yields a gain of about 200. Here the electron beam crosses the net photon beam at an angle of 1.3° . Scattered electrons are separated from the main electron beam which is bent by about 10.3° by dipole-3 in the chicane. The scattered electrons were detected using a multi-strip vapor deposited diamond detector which is illustrated in FIG. 1 and the scattered photons were detected in lead glass detector. The electron detector sits about 17mm (but can be moved perpendicular to the main electron beam) from the main electron beam but diamond detectors have been demonstrated to be radiation hard [26, 27]. Each strip builds a cumulative scattered electron count and therefore, over time an asymmetry number can be assigned to each strip 1.

Given the electron energy and photon energy, the Compton asymmetry in Eq. (2) can be calculated from theory [11]. Along with the knowledge of Compton asymmetry and polarization of the photons, the electron polarization can thus be measured to a high degree of precision. Here, the number of electrons seen by every strip of the electron detector individually translates to beam polarization. It might be interesting to note that, it is the number of electrons that were detected (by each strip individually) that is finally used to measure the asymmetry and not the final state electron energy or scattering angle. Such Compton polarimeters have been used in Jlab and SLAC and they have all fielded multi-strip electron detectors to improve statistics. Usually the polarization value obtained from each individual strip in the electron detector is averaged over or in some cases only a certain range of strips are selected for the measurement [13]. Surprisingly, even though only number of electrons counted per strip is used for polarization measurement and not the number distribution measured by all the strips on the whole, asymmetry distribution obtained from the number distribution is very sensitive to the value of speed of light.

3 Method

3.1 Determination of refractive index of free space

Usually the variation in speed of light is studied as a variation in the refractive index of vacuum. If the speed of light was constant w.r.t to a varying parameter, such as photon energy, the refractive index of vacuum is normalized to 1. For Compton scattering of electrons with initial energy ϵ_0 and mass m_e , on photons with initial and final energy and angle ω_0, θ_0 and ω, θ respectively, the Compton scattering cross section and longitudinal asymmetry are given by [8]:

$$\frac{d\sigma}{d\rho} = 2\pi r_e^2 a \left[\frac{\rho^2(1-a)^2}{1-\rho(1-a)} + 1 + \left(\frac{1-\rho(1+a)}{1-\rho(1-a)} \right)^2 \right] \quad (3)$$

$$A_l(\rho) = \frac{2\pi r_e^2 a}{d\sigma/d\rho} (1-\rho(1+a)) \left[1 - \frac{1}{(1-\rho(1-a))^2} \right] \quad (4)$$

Where $r_e = \alpha\hbar c/m_e c^2 = 2.817 \times 10^{-15}$ m, is the classical electron radius, $\rho = \omega/\omega_{max}$ is the scattered photon energy normalized to its maximum value, and $a = \frac{1}{1+4\omega_0\epsilon_0/m_e^2}$ is a kinematic parameter. As demonstrated in Ref. [7], Compton scattering is very sensitive to tiny deviations of the refractive index from unity due to an amplification of the effect by the square of the initial Lorentz boost (γ_0). For photons scattering off ultra-relativistic electrons in vacuum with $n \approx 1$ (up to $\mathcal{O}[(n-1)^2]$), energy-momentum conservation gives [9];

$$\epsilon_0 x - \omega(1 + x + \gamma_0^2 \theta^2) + 2\omega_0(1 - \frac{\omega}{\epsilon_0})\gamma_0^2(n - 1) = 0, \quad (5)$$

where $x = 4\gamma_0\omega_0 \sin^2(\frac{\theta_0^2}{2})/m_e$. The energy-momentum conservation equation (Eq. 5) can be re-written as;

$$\omega(n) = \frac{\epsilon_0 x}{1 + x + \gamma_0^2 \theta^2} \left(1 + \frac{2\gamma_0^2(n(\omega) - 1)(1 + \gamma_0^2 \theta^2)}{(1 + x + \gamma_0^2 \theta^2)^2} \right) \quad (6)$$

and the maximum energy of the scattered photon which occurs for $\theta = 0$ (called the Compton edge) is given by

$$\omega_{max}(n) = \frac{\epsilon_0 x}{1 + x} \left(1 + \frac{2\gamma_0^2(n(\omega_{max}) - 1)}{(1 + x)^2} \right) \quad (7)$$

In the Compton polarimeter, the scattered electrons are momentum analyzed by dipole-3 (see Fig. 2) and detected on a position sensitive detector which measures the deflection of the scattered electrons with respect to the unscattered electrons. The deflection of the electron can be calculated from the geometry and operating parameters of the dipole magnet. The vertical deflection for an electron incident on the i -th strip of the micro-strip detector is given by,

$$\begin{aligned} \Delta x_i &= [R_i(1 - \cos(\theta_i)) + z_i \tan(\theta_i)] \\ &- [R_0(1 - \cos(\theta_0)) + z_0 \tan(\theta_0)] \end{aligned} \quad (8)$$

where R_i, θ_i, z_i and R_0, θ_0, z_0 are the bend radius, bend angle and drift distance from the exit of the dipole to the detector plane, for the electrons incident on the i -th strip and the unscattered electron respectively. The bend radius of the unscattered electrons $R_0 = \frac{p_0}{eB} = \frac{L}{\sin(\theta_0)}$, where p_0 is the momentum of the electron beam, B is the magnitude of the dipole field and L is the length of the dipole. The bend radius of the scattered electrons incident on the i -th strip is given by $R_i = R_0 \left(\frac{p_i}{p_0} \right)$. Since the detector is inclined at an angle θ_{det} with respect to the vertical direction the deflection of an electron incident on the i -th strip along the detector plane is given by,

$$\Delta x_i^{det} = \frac{\Delta x_i \cos(\theta_0)}{\cos(\theta_{det} - \theta_0)} \quad (9)$$

A measurement of the electron deflection is a measurement of the scattered electron momentum, and since the momentum of the scattered electron is related to ρ via momentum conservation by,

$$p = p_0 + \omega_0 - \rho\omega_{max} \quad (10)$$

the measured electron deflection can be directly mapped to a value of ρ .

The electron detector used in the Hall-C Compton polarimeter has a strip pitch of 0.2 mm, for an electron incident on the i -th strip, its deflection along the detector plane is,

$$\Delta x_i^{det} = \Delta x_{max}^{det} - 0.2 * (N_{CE} - i), \quad (11)$$

where N_{CE} is the strip number where the Compton edge is located, Δx_{max}^{det} is the deflection of the electrons with minimum momentum, p_{min} , which correspond to the scattered photons with the maximum energy ω_{max} . The maximum deflection Δx_{max}^{det} can be calculated using Eqs. 8-10 for $\rho = 1$ and similarly by varying ρ between 0 – 1 in small steps a table of $\rho - \Delta x^{det}$ is built. The $\rho - \Delta x^{det}$ table is fit to a 4-th order polynomial and used to convert the measured Δx_i^{det} for the i -th detector strip to a corresponding ρ_i . This allows the measured longitudinal asymmetry as a function of detector strip-hit to be converted to a measured longitudinal asymmetry as a function of ρ . As mentioned earlier the measured longitudinal asymmetry is related to the calculated asymmetry (Eq. 4) according to Eq. 1. The measured asymmetry is fit to the calculated asymmetry (Eq. 4) with 2 free parameters, the $P_e P_\gamma$ the product of the electron and laser polarizations and N_{CE} the strip location of the Compton edge. The measured location of the Compton edge is then converted to ω_{max} , and using Eq. 7 the deviation of the refractive index from $n = 1$ for a photon energy of ω_{max} is calculated.

If the refractive index is independent of ω , the effect of any deviation of the refractive index from unity can be incorporated into the Compton cross section and longitudinal asymmetry by modifying the scattered photon energy normalized to its maximum value, $\rho \rightarrow \rho(n)$ as,

$$\rho(n) = \frac{\omega(n)}{\omega_{max}(n)} = \rho \left[\frac{1 + \frac{2\gamma_0^2(n-1)(1+\gamma_0^2\theta^2)}{(1+x+\gamma_0^2\theta^2)^2}}{1 + \frac{2\gamma_0^2(n-1)}{(1+x)^2}} \right]. \quad (12)$$

The above equation can be written up to $\mathcal{O}[(n-1)^2]$ as;

$$\rho(n) = \rho \left[1 + 2\gamma_0^2(n-1)f(x, \theta) \right], \quad (13)$$

where the kinematic function $f(x, \theta)$ is given by,

$$f(x, \theta) = \frac{(1 + \gamma_0^2\theta^2)(1+x)^2 - (1+x^2 + \gamma_0^2\theta^2)^2}{(1+x + \gamma_0^2\theta^2)^2(1+x)^2} \quad (14)$$

The longitudinal asymmetry can then be re-written to incorporate the deviation of the refractive index from $n = 1$ by replacing ρ by $\rho(n)$ in Eq. 4. The new modified asymmetry is then fit to the measured asymmetry with three parameters; the product of electron beam and laser polarizations, $P_e P_\gamma$, the strip location of the Compton edge, N_{CE} and $2\gamma_0^2(n-1)$. The new parameter $2\gamma_0^2(n-1)$ is used to extract the deviation of the refractive index from unity.

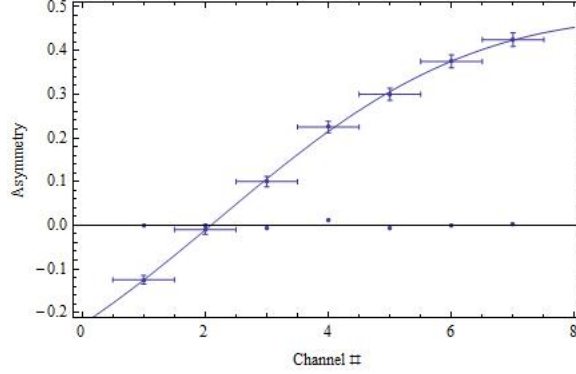


Figure 3: Plot showing a sample fit to Eq. (4) using data from a single strip read out from SLD Compton polarimeter.

Using the data of asymmetry measured at every channel for the JLab Hall-C Compton polarimeter, one could perform a least squares fit to the expression for asymmetry w.r.t the photon energy derived above in order to obtain values of n . The beam characteristics change over time, and therefore the Compton polarimeter data sets are limited to a fixed period of time to allow changes to be made. On fitting such data sets, a sample of which is illustrated in Fig. 3, we obtain a n for each data set. JLab Compton polarimeter ran for approximately 2 years and the extracted values of n is plotted w.r.t to run number (or data set) in FIG. 4.

3.2 Determination of limits on SME parameters

Minimal SME provides a number of ways to allow Lorentz and thus CPT violation [29]. The leading MSME coefficient which causes direction and polarization dependent speed of light is k_F [30]. In this sub section, we will try to impose limits on the $\tilde{\kappa}_{0+}$ components of κ_F , which is a 3×3 antisymmetric matrix. Using MSME, the dispersion relation for photon in terms of $\vec{\kappa}$ as;

$$\omega = (1 - \vec{\kappa} \cdot \hat{K})K + \mathcal{O}(\kappa^2) \quad (15)$$

$$\vec{\kappa} = \langle (\tilde{\kappa}_{0+}^{23}), (\tilde{\kappa}_{0+}^{31}), (\tilde{\kappa}_{0+}^{12}) \rangle = \langle \kappa_X, \kappa_Y, \kappa_Z \rangle \quad (16)$$

where ω is the energy of the photon, \vec{K} is the 3-momentum of the photon. Eq. 16 implies that the refractive index of free space is a function of $\vec{\kappa}$. Here Z-direction is parallel to the axes of rotation of the Earth. Using energy conservation in Compton scattering and Eq. 16, one could write the index of refraction of free space as;

$$n \approx \left(1 + \frac{2\gamma^2}{\left(1 + 4\gamma \frac{K}{m_e}\right)^2} \vec{\kappa} \cdot \hat{p} \right)$$

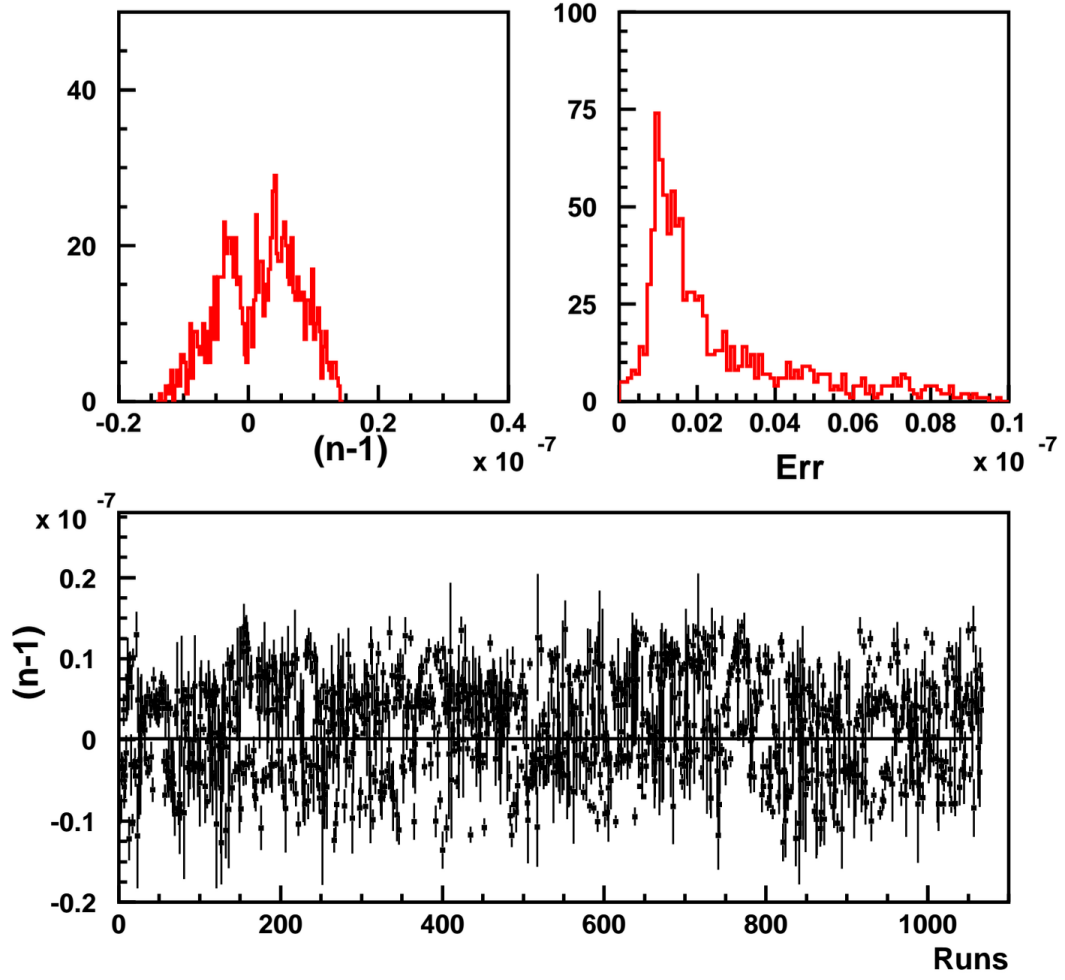


Figure 4: Plot showing the variation of ‘ $n - 1$ ’ as a function of simple time along with accrued errors when fit to a sinusoid.

$$n - 1 \approx 8.25 \times 10^6 \sqrt{\kappa_X^2 + \kappa_Y^2} \sin(\Omega t) \quad (17)$$

where $\hat{p}(t)$ is unit vector along the 3-momentum of electron beam which for QWeak was $\langle 0.13 \cos(\Omega t), 0.87 \sin(\Omega t), 0.48 \rangle$, $K = 2.32$ eV is the momentum of the photon beam, $|\vec{p}| = \epsilon_0 = 1.165$ GeV is the electron beam energy, $\gamma = 2280$ is the Lorentz boost of the electrons and $\Omega = 2\pi/(23h56m)$ is the frequency of rotation of the Earth. Finally Eq. 17 can be numerically expressed by disregarding the phase offset.

Furthermore, given that the JLab Compton polarimeter ran for almost 2 years, one could also study the variation of the refractive index of vacuum as a function of sidereal time and compare it to Eq. 17. Fig. 5 shows a plot of this variation fit to a pure sinusoid wave with a frequency of Ω , amplitude of $(0.3 \times 10^{-10} \pm 0.2 \times 10^{-9})$, an

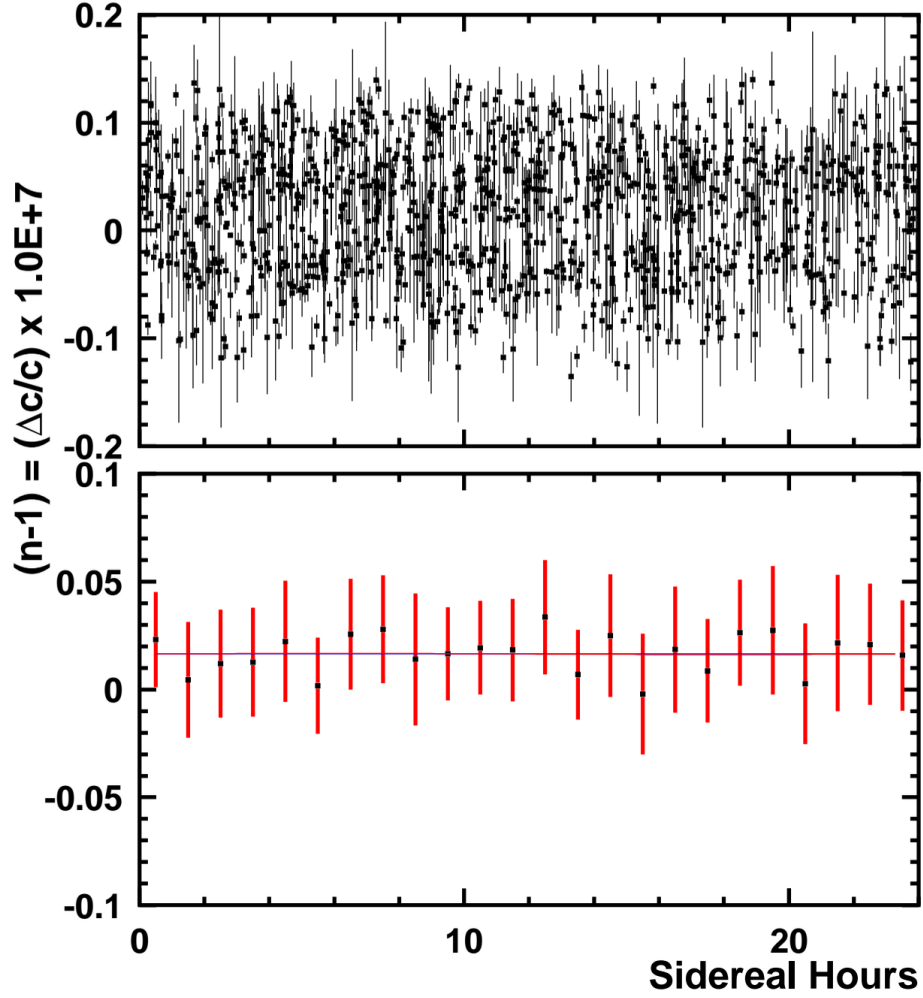


Figure 5: Plot showing the variation of ‘ $n - 1$ ’ as a function of sidereal time, with the entire data set from 1200 runs (2 years) rolled into modulo sidereal day.

offset of $(0.16 \times 10^{-8} \pm 0.02 \times 10^{-8})$, and with $\chi^2 = 1.24$ from 22 d.o.f. With a value of sinusoidal fit amplitude being limited to $< 0.2 \times 10^{-9}$, one could impose a limit on $\sqrt{\kappa_X^2 + \kappa_Y^2} < 2.4 \times 10^{-17}$ from Eq. 17.

4 Conclusion

Many other tests of CPT symmetry have nevertheless only solidified the case that Lorentz symmetry is indeed held good for a very large range of energy regime. In a dispersive medium whose refractive index is less than one, photons pair produce

and in medium whose refractive index is higher than one, charged particles undergo Cherenkov radiation dramatically reducing the maximum energy of these charged particles. Therefore highest energy charged cosmic particles detected and highest energy cosmic photon detected constrains variation of refractive index of vacuum w.r.t photon energy [14]. Cherenkov radiation and pair production are respectively forbidden if;

$$\begin{aligned}
|n - 1| &< \frac{m_{p(e)}^2}{2E_{p(e)}^2 - 2\omega_\gamma E_{p(e)} - m_{p(e)}^2} \\
&< \frac{2m_e^2}{\omega_\gamma^2}
\end{aligned} \tag{18}$$

On averaging the values of n obtained from the least squares fit to each data set in FIG. 4, we obtain a value of $n = 1 + (0.18 \times 10^{-9} \pm 0.02 \times 10^{-9})$. A limit of $\sqrt{\kappa_X^2 + \kappa_Y^2} < 2.4 \times 10^{-17}$ also implies that $\sqrt{(2c_{TX} - (\tilde{\kappa}_{0+}^{YZ})^2 + (2c_{TY} - (\tilde{\kappa}_{0+}^{ZX})^2} < 2.4 \times 10^{-17}$ [5].

References

- [1] C. S. Wu et. al., Physical Review **105** 4: 14131415 (1957).
- [2] J. H. Christenson, J. W. Cronin, V. L. Fitch, and R. Turlay, Phys. Rev. Lett. **13**, 138
- [3] O. W. Greenberg, Phys. Rev. Lett. **89**: 231602 (2002).
- [4] S. Liberati, Class. Quantum Grav. **30**: 133001 (2013).
- [5] V. A. Kosteleck and N. Russell, Rev. Mod. Phys. **83** 11 (2011).
- [6] W. Deconinck, Hyperfine Interactions **200** 1-3 (2011): 31-34.
- [7] V. Gharibyan, Phys. Lett. B **611**, 231 (2011).
- [8] F. W. Lipps and H. A. Tolhoek, Physica **20** 85: 385 (1954).
- [9] V. Gharibyan, Phys. Rev. Lett. **109**: 141103 (2012).
- [10] V. Gharibyan, arXiv:1401.3720
- [11] S. C. Miller and R. M. Wilcox, Phys. Rev. Lett **124**, 3 (1961).
- [12] I. F. Ginzburg, et. al. , Nucl. Instrum. Methods A **219**, 5 (1984).

- [13] R. C. King, SLAC Technical Report **0452**.
- [14] S. Coleman and S. L. Glashow, Phys. Lett. B **405**, (1997): 249.
- [15] D. Androic et al., Phys. Rev. Lett. **111**, 141803 (2013).
- [16] T. Allison et al., Nucl. Instr. Meth. **A781**,105 (2015).
- [17] D. Gustavson et al., Nucl. Instr. Meth. **A165**, 177 (1979)
- [18] L. Knudsen et al., Phys. Lett. **B270**, 97 (1991).
- [19] D. P. Barber et al., Nucl. Instr. Meth. **A329**, 79 (1993).
- [20] I. Passchier et al., Nucl. Instr. Meth. **A414**, 446 (1998).
- [21] W. Franklin et al., AIP Conf.Proc. **675**, 1058 (2003).
- [22] M. Baylac et al., Phys. Lett. **B539**, 8 (2002); N. Felletto et al., Nucl. Instr. Meth. **A459**, 412 (2001).
- [23] M. Friend et al., Nucl. Instr. Meth. **A676**, 96 (2012).
- [24] K. Abe et al., Phys. Rev. Lett. **84**, 5945 (2000); M. Woods, hep-ex/9611005 (1996).
- [25] A. Acha et al. [HAPPEX Collab.], Phys. Rev. Lett. **98**, 032301 (2007).
- [26] C. Bauer et al., Nucl. Instrum. Methods **367**, 207 (1995).
- [27] M. M. Zoeller et al., IEEE Trans. Nucl. Sci. **44**, 815 (1997).
- [28] A. Denner and S. Dittmaier, Nucl. Phys. **B540**, 58 (1999).
- [29] M. A. Hohensee et al., Phys. Rev. Lett. **102**, 170402 (2009); Phys. Rev. **D 80**, 036010 (2009); B. D. Altschul, Phys. Rev. **D 80**, 091901(R) (2009).
- [30] V. A. Kostelecky and M. Mewes, Phys. Rev. Lett. **87**, 251304 (2001); Phys. Rev. **D 66**, 056005 (2002).